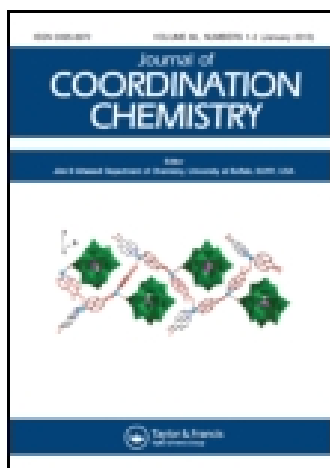


This article was downloaded by: [Institute Of Atmospheric Physics]
On: 09 December 2014, At: 15:23
Publisher: Taylor & Francis
Informa Ltd Registered in England and Wales Registered Number: 1072954 Registered office: Mortimer House, 37-41 Mortimer Street, London W1T 3JH, UK



Journal of Coordination Chemistry

Publication details, including instructions for authors and subscription information:

<http://www.tandfonline.com/loi/gcoo20>

Synthetic and structural studies of dicobalt-iron complexes with intramolecular bridging bidentate ligands

Xu-Feng Liu^a & Xie Li^a

^a Department of Chemical Engineering, Center of Analysis and Testing, Ningbo University of Technology, Ningbo, China

Accepted author version posted online: 03 Sep 2014. Published online: 23 Sep 2014.



[Click for updates](#)

To cite this article: Xu-Feng Liu & Xie Li (2014) Synthetic and structural studies of dicobalt-iron complexes with intramolecular bridging bidentate ligands, Journal of Coordination Chemistry, 67:19, 3226-3233, DOI: [10.1080/00958972.2014.961443](https://doi.org/10.1080/00958972.2014.961443)

To link to this article: <http://dx.doi.org/10.1080/00958972.2014.961443>

PLEASE SCROLL DOWN FOR ARTICLE

Taylor & Francis makes every effort to ensure the accuracy of all the information (the "Content") contained in the publications on our platform. However, Taylor & Francis, our agents, and our licensors make no representations or warranties whatsoever as to the accuracy, completeness, or suitability for any purpose of the Content. Any opinions and views expressed in this publication are the opinions and views of the authors, and are not the views of or endorsed by Taylor & Francis. The accuracy of the Content should not be relied upon and should be independently verified with primary sources of information. Taylor and Francis shall not be liable for any losses, actions, claims, proceedings, demands, costs, expenses, damages, and other liabilities whatsoever or howsoever caused arising directly or indirectly in connection with, in relation to or arising out of the use of the Content.

This article may be used for research, teaching, and private study purposes. Any substantial or systematic reproduction, redistribution, reselling, loan, sub-licensing, systematic supply, or distribution in any form to anyone is expressly forbidden. Terms &

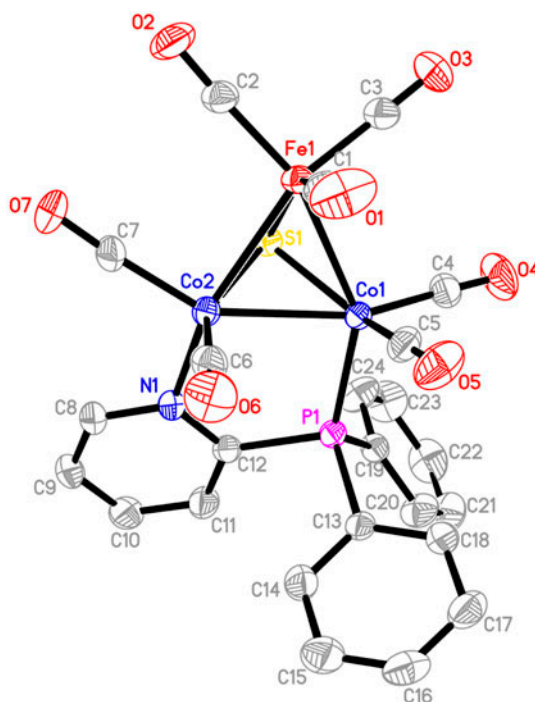
Conditions of access and use can be found at <http://www.tandfonline.com/page/terms-and-conditions>

Synthetic and structural studies of dicobalt–iron complexes with intramolecular bridging bidentate ligands

XU-FENG LIU* and XIE LI

Department of Chemical Engineering, Center of Analysis and Testing, Ningbo University of Technology, Ningbo, China

(Received 27 June 2014; accepted 16 August 2014)



Treatment of $(\mu_3\text{-S})\text{FeCo}_2(\text{CO})_9$ (**1**) with diphenyl-2-pyridylphosphine ($2\text{-C}_5\text{H}_4\text{NPPh}_2$) or $\text{Ph}_2\text{PN}(\text{CH}_2\text{CHMe}_2)\text{PPh}_2$ at reflux in toluene resulted in the formation of dicobalt–iron complexes $(\mu_3\text{-S})\text{FeCo}_2(\text{CO})_7(2\text{-C}_5\text{H}_4\text{NPPh}_2)$ (**2**) and $(\mu_3\text{-S})\text{FeCo}_2(\text{CO})_7[\text{Ph}_2\text{PN}(\text{CH}_2\text{CHMe}_2)\text{PPh}_2]$ (**3**) with bridging bidentate ligands via carbonyl substitution in 51 and 53% yields, respectively. The new complexes **2** and **3** were structurally characterized by elemental analysis, IR and NMR spectroscopy, and X-ray crystallography.

Keywords: Dicobalt–iron; Bidentate ligand; Carbonyl substitution; Synthesis; Crystal structure

*Corresponding author. Email: nkxfliu@126.com

1. Introduction

Carbonyl substitution reactions of the metal carbonyl complexes with monodentate or bidentate ligands have attracted interest in organometallic chemistry, because these reactions are easily undertaken and the target products have interesting properties [1–6]. Previous studies revealed that the carbonyls bound to cobalt of $(\mu_3\text{-S})\text{FeCo}_2(\text{CO})_9$ are more easily exchanged by phosphine ligands than the carbonyls bound to iron [7]. We previously reported the carbonyl substitution reactions of $(\mu_3\text{-S})\text{FeCo}_2(\text{CO})_9$ (**1**) with diphosphine ligands afforded three coordination modes [8–10]: intramolecular bridging, such as $(\mu_3\text{-S})\text{FeCo}_2(\text{CO})_7[\text{Ph}_2\text{PN}(\text{R})\text{PPh}_2]$ (R = $\text{CH}_2\text{CH}_2\text{CH}_3$, CH_2Ph), $(\mu_3\text{-S})\text{FeCo}_2(\text{CO})_7(\text{Ph}_2\text{PCH}_2\text{PPh}_2)$, and $(\mu_3\text{-S})\text{FeCo}_2(\text{CO})_7(\text{Ph}_2\text{PCH}_2\text{CH}_2\text{PPh}_2)$; intermolecular bridging, such as $[(\mu_3\text{-S})\text{FeCo}_2(\text{CO})_8]_2(\text{Ph}_2\text{PCH}_2\text{CH}_2\text{PPh}_2)$ and $[(\mu_3\text{-S})\text{FeCo}_2(\text{CO})_8]_2(\text{Ph}_2\text{PCH}_2\text{CH}_2\text{CH}_2\text{CH}_2\text{PPh}_2)$; chelating, such as $(\mu_3\text{-S})\text{FeCo}_2(\text{CO})_7(\text{cis-Ph}_2\text{PCH}=\text{CHPPh}_2)$. Recently, we carried out a study of the carbonyl substitution reaction of **1** with diphenyl-2-pyridylphosphine, and we have prepared the intramolecular bridging dicobalt–iron complex $(\mu_3\text{-S})\text{FeCo}_2(\text{CO})_7(2\text{-C}_5\text{H}_4\text{NPPH}_2)$ (**2**). In addition, N-substituted bis(diphenylphosphanyl)amine coordinated complex $(\mu_3\text{-S})\text{FeCo}_2(\text{CO})_7[\text{Ph}_2\text{PN}(\text{CH}_2\text{CHMe}_2)\text{PPh}_2]$ (**3**) was also produced by the carbonyl exchange reaction. In this paper, we report the synthesis and crystal structures of the dicobalt–iron complexes **2** and **3** containing bridging bidentate ligands $2\text{-C}_5\text{H}_4\text{NPPH}_2$ or $\text{Ph}_2\text{PN}(\text{CH}_2\text{CHMe}_2)\text{PPh}_2$.

2. Experimental

2.1. Materials and methods

All reactions were performed using standard Schlenk and vacuum line techniques under N_2 . Toluene was distilled over sodium under N_2 . $2\text{-C}_5\text{H}_4\text{NPPH}_2$ and other materials were available commercially and used as received. Complex **1** [11] and $\text{Ph}_2\text{PN}(\text{CH}_2\text{CHMe}_2)\text{PPh}_2$ [12] were prepared according to literature procedures. IR spectra were recorded on a Nicolet MAGNA 560 FTIR spectrometer. NMR spectra were obtained on a Bruker Avance 500 MHz spectrometer. Elemental analyses were performed by a Perkin-Elmer 240C analyzer.

2.2. Synthesis of $(\mu_3\text{-S})\text{FeCo}_2(\text{CO})_7(2\text{-C}_5\text{H}_4\text{NPPH}_2)$ (**2**)

A solution of **1** (0.092 g, 0.2 mM) and $2\text{-C}_5\text{H}_4\text{NPPH}_2$ (0.053 g, 0.2 mM) in toluene (10 mL) was refluxed for 0.5 h. The solvent was reduced *in vacuo* and the residue was subjected to TLC separation using $\text{CH}_2\text{Cl}_2/\text{petroleum ether}$ (v/v = 1 : 2), as eluent. From the main brown band, 0.068 g (51%) of **2** was obtained as a black solid. Anal. Calcd for $\text{C}_{24}\text{H}_{14}\text{Co}_2\text{FeNO}_7\text{PS}$: C, 43.34; H, 2.12; N, 2.11. Found: C, 43.71; H, 2.32; N, 1.98. IR (KBr disk, cm^{-1}): $\nu_{\text{C}\equiv\text{O}}$ 2051 (vs), 2005 (vs), 1989 (vs), 1939 (vs), and 1922 (vs). ^1H NMR (500 MHz, CDCl_3): 8.95 (d, $J = 5.0$ Hz, 1H, PyH), 7.92–7.88 (m, 2H, PhH), 7.67–7.63 (m, 2H, PhH), 7.48 (s, 6H, PhH), 7.13–7.08 (m, 2H, PyH), and 6.86 (d, $J = 8.0$ Hz, 1H, PyH) ppm. $^{31}\text{P}\{^1\text{H}\}$ NMR (200 MHz, CDCl_3 , 85% H_3PO_4): 37.54 (s) ppm. $^{13}\text{C}\{^1\text{H}\}$ NMR (125 MHz, CDCl_3): 213.02 (C \equiv O), 167.27 (d, $J_{\text{P-C}} = 61.2$ Hz, 2-PyC), 156.09 (d, $J_{\text{P-C}} = 13.1$ Hz, 6-PyC), 136.11 (d, $J_{\text{P-C}} = 3.1$ Hz, 4-PyC), 134.40 (d, $J_{\text{P-C}} = 34.6$ Hz,

i-PhC), 133.40 (d, $J_{P-C} = 12.6$ Hz, *o*-PhC), 131.33 (d, $J_{P-C} = 11.2$ Hz, 3-PyC), 131.01 (d, $J_{P-C} = 1.4$ Hz, *p*-PhC), 130.54 (d, $J_{P-C} = 1.5$ Hz, *p*-PhC), 129.17 (t, $J_{P-C} = 10.2$ Hz, *m*-PhC), and 125.61 (s, 5-PyC) ppm.

2.3. Synthesis of $(\mu_3-S)FeCo_2(CO)_7[Ph_2PN(CH_2CHMe_2)PPh_2]$ (**3**)

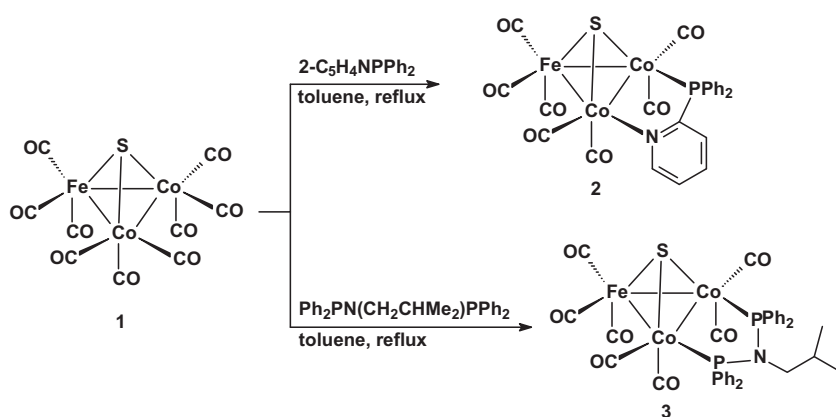
A solution of **1** (0.092 g, 0.2 mM) and $Ph_2PN(CH_2CHMe_2)PPh_2$ (0.088 g, 0.2 mM) in toluene (10 mL) was refluxed for 0.5 h. The solvent was reduced *in vacuo* and the residue was subjected to TLC separation using CH_2Cl_2 /petroleum ether (*v/v* = 1 : 5) as eluent. From the main brown band, we obtained 0.089 g (53%) of **3** as a black solid. Anal. Calcd for $C_{35}H_{29}Co_2FeNO_7P_2S$: C, 49.85; H, 3.47; N, 1.66. Found: C, 49.76; H, 3.70; N, 1.61. IR (KBr disk, cm^{-1}): $\nu_{C=O}$ 2051 (vs), 2011 (vs), 1992 (vs), 1961 (vs), 1947 (vs), and 1933 (vs). 1H NMR (500 MHz, $CDCl_3$): 7.70 (s, 8H, PhH), 7.53 (s, 12H, PhH), 2.43 (q, $J = 7$ Hz, 2H, CH_2), 1.31–1.30 (m, 1H, CH), and –0.05 (d, $J = 6.5$ Hz, 6H, $2CH_3$) ppm. $^{31}P\{^1H\}$ NMR (200 MHz, $CDCl_3$, 85% H_3PO_4): 105.48 (s) ppm. $^{13}C\{^1H\}$ NMR (125 MHz, $CDCl_3$): 213.58 (C=O), 136.77 (d, $J_{P-C} = 46.6$ Hz, *i*-PhC), 136.02 (d, $J_{P-C} = 45.4$ Hz, *i*-PhC), 132.41 (t, $J_{P-C} = 6.2$ Hz, *o*-PhC), 131.68 (t, $J_{P-C} = 6.5$ Hz, *o*-PhC), 130.91, 130.84 (2s, *p*-PhC), 128.75 (t, $J_{P-C} = 5.0$ Hz, *m*-PhC), 128.43 (t, $J_{P-C} = 4.9$ Hz, *m*-PhC), 60.19 (t, $J_{P-C} = 5.4$ Hz, CH_2), 26.45 (s, CH), and 19.23 (s, CH_3) ppm.

Table 1. Crystal data and structure refinement details for **2** and **3**.

Complex	2	3
Empirical formula	$C_{24}H_{14}Co_2FeNO_7PS$	$C_{35}H_{29}Co_2FeNO_7P_2S$
Formula weight	665.10	843.30
Temperature (K)	294(2)	294(2)
Wavelength (Å)	0.71073	0.71073
Crystal system	Orthorhombic	Triclinic
Space group	$P2(1)2(1)2(1)$	$P-1$
<i>a</i> (Å)	10.919(5)	12.10(3)
<i>b</i> (Å)	15.092(7)	13.57(4)
<i>c</i> (Å)	16.025(7)	13.80(5)
α (°)	90	83.01(10)
β (°)	90	67.64(8)
γ (°)	90	80.02(12)
<i>V</i> (Å ³)	2641(2)	2059(11)
<i>Z</i>	4	2
D_{calcd} (g cm ⁻³)	1.673	1.360
μ (mm ⁻¹)	1.967	1.314
<i>F</i> (0 0 0)	1328	856
Crystal size (mm ³)	0.42 × 0.23 × 0.16	0.41 × 0.23 × 0.03
θ_{min} , θ_{max} (°)	3.15, 27.47	3.05, 25.03
Reflections collected/unique	27,374/5969	17,661/7253
R_{int}	0.0675	0.0754
<i>hkl</i> range	–14 ≤ <i>h</i> ≤ 14 –19 ≤ <i>k</i> ≤ 19 –20 ≤ <i>l</i> ≤ 20	–14 ≤ <i>h</i> ≤ 14 –16 ≤ <i>k</i> ≤ 16 –16 ≤ <i>l</i> ≤ 16
Completeness to θ_{max} (%)	98.7	99.5
Data/restraints/parameters	5969/0/334	7253/0/444
Goodness of fit on F^2	0.876	1.116
R_1/wR_2 ($I > 2\sigma(I)$)	0.0307/0.0577	0.0712/0.2161
R_1/wR_2 (all data)	0.0374/0.0614	0.0916/0.2391
Largest diff. peak and hole (e Å ⁻³)	0.356/–0.314	1.261/–0.524

2.4. X-ray structure determination

Single crystals of **2** and **3** suitable for X-ray diffraction analysis were grown by slow evaporation of CH_2Cl_2 /hexane solutions of **2** and **3** at 4 °C. A single crystal of **2** or **3** was mounted on a Rigaku MM-007 CCD diffractometer. Data were collected at 294 K using a graphite monochromator with Mo $K\alpha$ radiation ($\lambda = 0.71073 \text{ \AA}$) in the ω - ϕ scanning mode. Data collection, reduction, and absorption correction were performed by the *CRYSTAL-CLEAR* program [13]. The structure was solved by direct methods using SHELXS-97 [14] and refined by full-matrix least-squares (SHELXL-97) [15] on F^2 . Hydrogens were located using the geometric method. Details of crystal data, data collections, and structure refinement are summarized in table 1.



Scheme 1. Preparation of **2** and **3**.

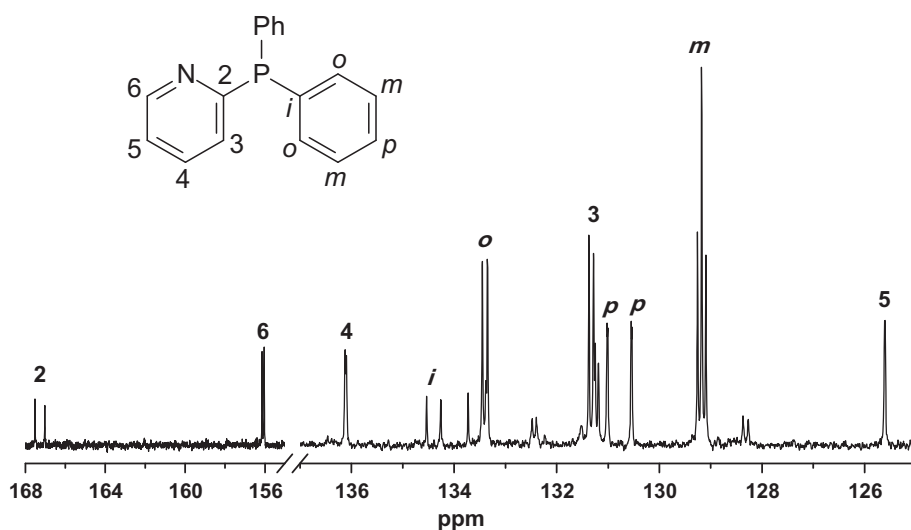


Figure 1. The $^{13}\text{C}\{^1\text{H}\}$ NMR spectra of **2** (168–125 ppm).

3. Results and discussion

3.1. Synthesis and characterization

Reactions of **1** with the bidentate ligands 2-C₅H₄NPPh₂ or Ph₂PN(CH₂CHMe₂)PPh₂ at reflux in toluene for 0.5 h resulted in the formation of **2** and **3** with intramolecular bridging bidentate ligand in 51 and 53% yields, respectively (scheme 1).

The new complexes **2** and **3** are air-stable black solids, characterized by elemental analysis and spectroscopy. The IR spectra of **2** and **3** showed five to six absorptions at 2051–1922 cm⁻¹ assigned to their seven terminal carbonyls, and the values are moved to lower frequencies with respect to those of **1** (2106, 2067, 2054, 2041, 2029, and 1973 cm⁻¹), [11] because the bidentate ligands have stronger electron-donating properties than carbonyl. The ¹H NMR spectra of **2** displayed two doublets at δ 8.95 and 6.86 ppm and a multiplet at δ 7.13–7.08 ppm for the pyridyl protons and two multiplets at δ 7.92–7.88 and 7.67–7.63 ppm for the phenyl protons, whereas the ¹H NMR spectra of **3** displayed two singlets at δ 7.70 and 7.53 ppm for the phenyl protons. The ³¹P{¹H} NMR spectra of **3** exhibited a singlet at δ 105.48 ppm for the two symmetrical phosphorus atoms of Ph₂PN(CH₂CHMe₂)PPh₂ coordinated to cobalt. The

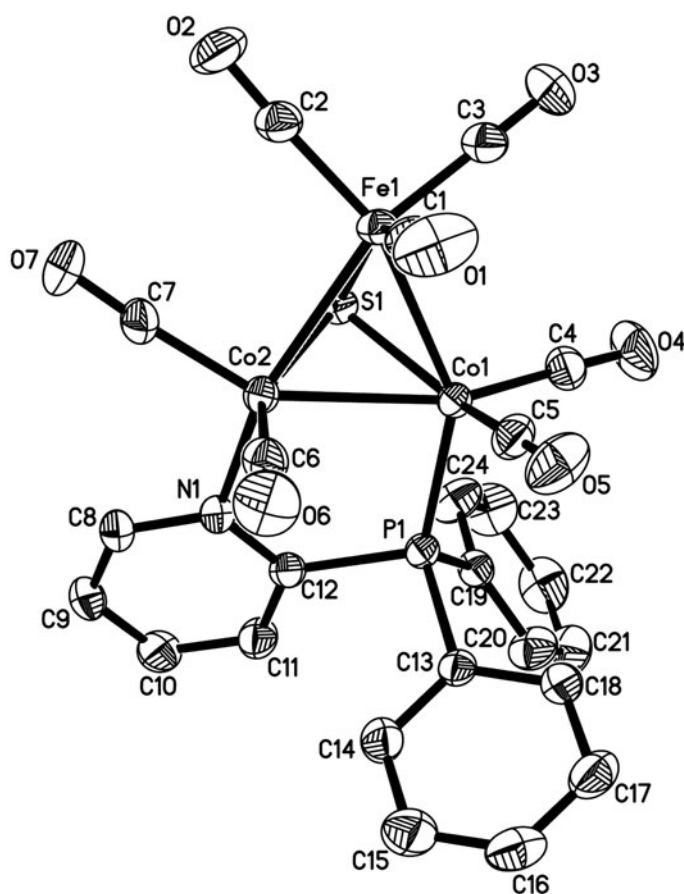


Figure 2. ORTEP view of **2** with 30% probability ellipsoids.

$^{13}\text{C}\{^1\text{H}\}$ NMR spectrum of **2** is shown in figure 1. We assigned the signals of the pyridyl and phenyl carbons in detail according to their chemical shifts and coupling constants.

3.2. X-ray crystal structures

The molecular structures of **2** and **3** were determined by single-crystal X-ray diffraction analysis. While ORTEP views of **2** and **3** are shown in figures 2 and 3, selected bond lengths and angles are presented in table 2. Complex **2** crystallizes in the orthorhombic space group $P2(1)2(1)2(1)$ with four molecules in the unit cell and one molecule in the asymmetric unit. As shown in figure 2, **2** consists of a dicobalt–iron triangle cluster with a $\mu_3\text{-S}$, seven terminal carbonyls, and an intramolecular bridging $2\text{-C}_5\text{H}_4\text{NPPh}_2$. The phosphorus and nitrogen of $2\text{-C}_5\text{H}_4\text{NPPh}_2$ attached to Co1 and Co2 are located in a basal–basal position of the square-pyramidal coordination sphere around Co1 and Co2, consistent with the crystal structures of $(\mu_3\text{-S})\text{FeCo}_2(\text{CO})_7[\text{Ph}_2\text{PN}(\text{R})\text{PPh}_2]$ ($\text{R} = \text{CH}_2\text{CH}_2\text{CH}_3$, CH_2Ph), [8] but different from the crystal structures of $(\mu_3\text{-S})\text{FeCo}_2(\text{CO})_8(\text{PPh}_3)$ and $[(\mu_3\text{-S})\text{FeCo}_2(\text{CO})_8]_2(\text{Ph}_2\text{PCH}_2\text{CH}_2\text{CH}_2\text{CH}_2\text{PPh}_2)$ [10]. The five-membered metallocycle Co1Co2N1C12P1 is nearly coplanar with mean deviation of 0.1218 Å from the plane. The average

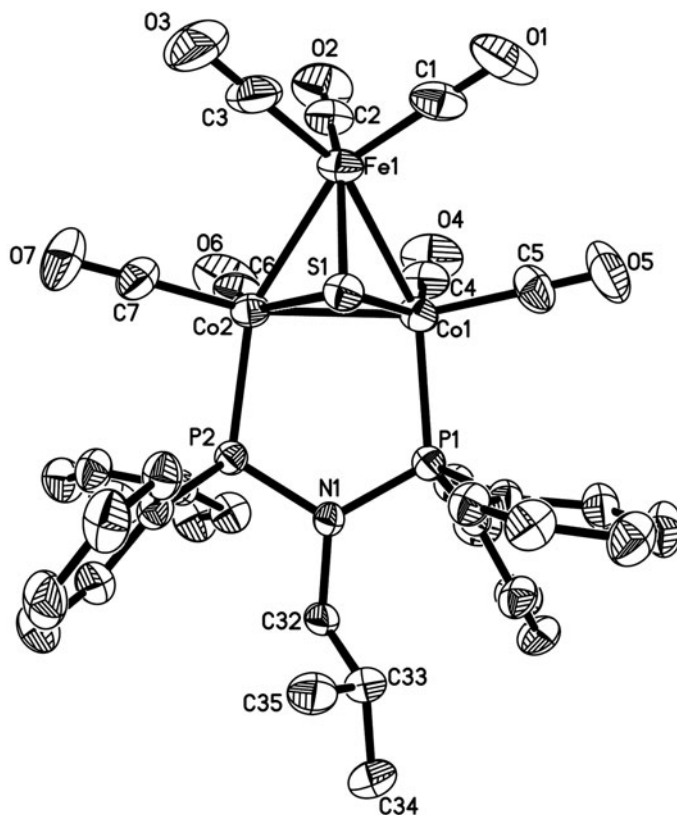


Figure 3. ORTEP view of **3** with 30% probability ellipsoids.

Table 2. Selected bond lengths (Å) and angles (°) for **2** and **3**.

2			
Fe(1)–S(1)	2.1754(11)	Co(1)–P(1)	2.1953(13)
Fe(1)–Co(1)	2.5403(11)	Co(1)–Co(2)	2.5064(10)
Fe(1)–Co(2)	2.5668(10)	Co(2)–N(1)	2.044(3)
Co(1)–S(1)	2.1655(12)	Co(2)–S(1)	2.1657(12)
S(1)–Fe(1)–Co(1)	54.00(3)	P(1)–Co(1)–Co(2)	86.91(3)
S(1)–Fe(1)–Co(2)	53.58(3)	S(1)–Co(1)–Fe(1)	54.36(3)
Co(1)–Fe(1)–Co(2)	58.78(3)	P(1)–Co(1)–Fe(1)	147.15(3)
S(1)–Co(1)–P(1)	102.08(4)	Co(2)–Co(1)–Fe(1)	61.14(2)
S(1)–Co(1)–Co(2)	54.65(3)	Co(1)–Co(2)–Fe(1)	60.08(2)
3			
Co(1)–S(1)	2.181(8)	Co(2)–S(1)	2.171(7)
Co(1)–P(1)	2.224(7)	Co(2)–P(2)	2.205(7)
Co(1)–Co(2)	2.499(7)	Co(2)–Fe(1)	2.547(6)
Co(1)–Fe(1)	2.557(6)	Fe(1)–S(1)	2.165(6)
S(1)–Co(1)–Co(2)	54.8(2)	P(2)–Co(2)–Co(1)	96.15(13)
P(1)–Co(1)–Co(2)	95.13(13)	Co(1)–Co(2)–Fe(1)	60.88(14)
S(1)–Co(1)–Fe(1)	53.66(17)	S(1)–Fe(1)–Co(2)	54.1(2)
Co(2)–Co(1)–Fe(1)	60.47(17)	S(1)–Fe(1)–Co(1)	54.3(2)
S(1)–Co(2)–Co(1)	55.1(2)	Co(2)–Fe(1)–Co(1)	58.65(17)

M–M bond length (2.5378 Å) is slightly shorter than that of **1** (2.557 Å) [16]. The average M–S bond length (2.1689 Å) is slightly longer than that of **1** (2.158 Å) [16].

Complex **3** crystallizes in the triclinic space group *P*-1 with two molecules in the unit cell and one molecule in the asymmetric unit. As shown in figure 3, **3** consists of a dicobalt–iron triangle cluster with a μ_3 -S, seven terminal carbonyls and an intramolecular bridging Ph₂PN(CH₂CHMe₂)PPh₂. The two phosphorus atoms of Ph₂PN(CH₂CHMe₂)PPh₂ reside in a basal–basal position of the square-pyramidal coordination sphere of cobalt, which is similar to **2**. The average M–M bond length (2.5343 Å) and M–S bond length (2.1723 Å) are comparable to those of **2**.

4. Conclusion

The dicobalt–iron complexes **2** and **3** containing intramolecular bridging bidentate ligands have been prepared by the carbonyl substitution reactions. Complex **2** and **3** were characterized by elemental analysis, IR and NMR spectroscopy. In addition, the molecular structures of **2** and **3** were confirmed by X-ray diffraction analysis, indicating that the bidentate ligands 2-C₅H₄NPPH₂ or Ph₂PN(CH₂CHMe₂)PPh₂ coordinate with the two cobalts of the dicobalt–iron cluster.

Supplementary material

CCDC 1009634 (**2**) and 1009635 (**3**) contain the supplementary crystallographic data for this paper. These data can be obtained free of charge from The Cambridge Crystallographic Data Center via www.ccdc.cam.ac.uk/data_request/cif.

Funding

National Training Programs of Innovation and Entrepreneurship for Undergraduates [grant number 201311058010]; the Zhejiang Province Science and Technology Innovation Program [grant number 2013R422014]; and the Ningbo Science and Technology Innovation Team [grant number 2011B82002].

References

- [1] (a) S. Ghosh, G. Hogarth, N. Hollingsworth, K.B. Holt, I. Richards, M.G. Sanchez, D. Unwin. *Dalton Trans.*, **42**, 6775 (2013); (b) N. Wang, M. Wang, L. Chen, L. Sun. *Dalton Trans.*, **42**, 12059 (2013); (c) C.A. Mebi, D.S. Karr, B.C. Noll. *Polyhedron*, **50**, 164 (2013); (d) C.-G. Li, Y. Zhu, X.-X. Jiao, X.-Q. Fu. *Polyhedron*, **67**, 416 (2014).
- [2] (a) S. Ezzaher, J.-F. Capon, F. Gloaguen, F.Y. Pétillon, P. Schollhammer, J. Talarmin. *Inorg. Chem.*, **46**, 9863 (2007); (b) D. Chouffai, G. Zampella, J.-F. Capon, L. De Gioia, A. Le Goff, F.Y. Pétillon, P. Schollhammer, J. Talarmin. *Organometallics*, **31**, 1082 (2012); (c) S. Ezzaher, J.-F. Capon, F. Gloaguen, F.Y. Pétillon, P. Schollhammer, J. Talarmin. *Inorg. Chem.*, **48**, 2 (2009); (d) P.-H. Zhao, X.-H. Li, Y.-F. Liu, Y.-Q. Liu. *J. Coord. Chem.*, **67**, 766 (2014).
- [3] (a) S. Ghosh, G. Hogarth, N. Hollingsworth, K.B. Holt, S.E. Kabir, B.E. Sanchez. *Chem. Commun.*, **50**, 945 (2014); (b) F.I. Adam, G. Hogarth, I. Richards, B.E. Sanchez. *Dalton Trans.*, 2495 (2007); (c) G. Hogarth, S.E. Kabir, I. Richards. *Organometallics*, **29**, 6559 (2010); (d) P.-H. Zhao, Y.-Q. Liu, G.-Z. Zhao. *Polyhedron*, **53**, 144 (2013).
- [4] (a) M. El-khateeb, M. Harb, Q. Abu-Salem, H. Görls, W. Weigand. *Polyhedron*, **61**, 1 (2013); (b) T.-H. Yen, K.-T. Chu, W.-W. Chiu, Y.-C. Chien, G.-H. Lee, M.-H. Chiang. *Polyhedron*, **64**, 247 (2013); (c) S. Gao, H. Guo, X. Peng, X. Zhao, Q. Duan, Q. Liang, D. Jiang. *New J. Chem.*, **37**, 1437 (2013); (d) P.-Y. Orain, J.-F. Capon, N. Kervaree, F. Gloaguen, F.Y. Pétillon, R. Pichon, P. Schollhammer, J. Talarmin. *Dalton Trans.*, 3754 (2007).
- [5] (a) X.-F. Liu, B.-S. Yin. *J. Coord. Chem.*, **63**, 4061 (2010); (b) X.-F. Liu, X.-W. Xiao. *J. Organomet. Chem.*, **696**, 2767 (2011); (c) X.-F. Liu, Z.-Q. Jiang, Z.-J. Jia. *Polyhedron*, **33**, 166 (2012); (d) X.-F. Liu, X.-Y. Yu, H.-Q. Gao. *Mol. Cryst. Liq. Cryst.*, **592**, 229 (2014).
- [6] (a) X.-F. Liu, H.-Q. Gao. *J. Clust. Sci.*, **25**, 367 (2014); (b) X.-F. Liu, H.-Q. Gao. *J. Clust. Sci.*, **25**, 495 (2014); (c) X.-F. Liu. *Polyhedron*, **72**, 66 (2014); (d) X.-F. Liu. *J. Organomet. Chem.*, **750**, 117 (2014).
- [7] (a) L.-M. Han, Q.-L. Suo, Y.-B. Wang, J.-H. Ye, N. Zhu, X.-B. Leng, J. Sun. *Polyhedron*, **24**, 759 (2005); (b) S.G. Bott, J. Wang, H. Shen, M.G. Richmond. *J. Chem. Crystallogr.*, **29**, 391 (1999).
- [8] L.-J. Luo, X.-F. Liu, H.-Q. Gao. *J. Coord. Chem.*, **66**, 1077 (2013).
- [9] X.-F. Liu, H.-Q. Gao. *Polyhedron*, **65**, 1 (2013).
- [10] X.-F. Liu, M.-Y. Chen, H.-Q. Gao. *J. Coord. Chem.*, **67**, 57 (2014).
- [11] M. Cowie, R.L. Dekock, T.R. Wagenmaker, D. Seyferth, R.S. Henderson, M.K. Gallagher. *Organometallics*, **8**, 119 (1989).
- [12] X.-F. Liu. *Inorg. Chim. Acta*, **421**, 10 (2014).
- [13] CrystalClear and CrystalStructure, Rigaku and Rigaku Americas, The Woodlands, TX (2007).
- [14] G.M. Sheldrick. *SHELXS97, A Program for Crystal Structure Solution*, University of Göttingen, Germany (1997).
- [15] G.M. Sheldrick. *SHELXL97, A Program for Crystal Structure Refinement*, University of Göttingen, Germany (1997).
- [16] D.L. Stevenson, C.H. Wei, L.F. Dahl. *J. Am. Chem. Soc.*, **93**, 6027 (1971).